Improvement of visible light photocatalytic acetaldehyde decomposition of bismuth vanadate/silica nanocomposites by cocatalyst loading

Improvement of visible light photocatalytic activity of bismuth vanadate/silica nanocomposites by cocatalyst loading

Naoya Murakami, Naohiro Takebe, Toshiki Tshubota and Teruhisa Ohno*

Department of Applied Chemistry, Faculty of Engineering, Kyushu Institute of Technology, 1-1 Sensuicho, Tobata, Kitakyushu 804-8550, Japan

Abstract

   Photocatalytic activity of bismuth vanadate ($BiVO_4$) for acetaldehyde decomposition under visible light irradiation was improved by inclusion of a nanocomposition of silica as an adsorbent material and loading of platinum (Pt) and trivalent iron ion (Fe^{3+}) as reduction cocatalysts. Addition of silica enhanced photocatalytic activity due to improvement of adsorption ability, but total decomposition of acetaldehyde was not observed within 24 h of visible light irradiation.   For further improvement of photocatalytic activity, Pt and Fe^{3+} were modified on $BiVO_4$ with an optimized amount of silica composition.   Photodeposition of Pt greatly increased photocatalytic activity, and acetaldehyde was totally decomposed within 24 h of visible light irradiation.

Keywords: Visible-light responsive photocatalyst; Bismuth vanadate; Silica; Reduction cocatalyst.

* Corresponding author. TEL/FAX: +81-93-884-3318

E-mail address: tohno@che.kyutech.ac.jp (T. Ohno)

1. Introduction

Many studies have been conducted over the past few decades on semiconductor photocatalysts as sustainable material for environmental remediation.   Titanium(IV) oxide (TiO_2) is the most appropriate material for a photocatalyst because of its excellent properties, such as its high chemical stability, nontoxicity, and high oxidation ability [1,2].   However, one drawback is that photocatalytic reaction over TiO_2 requires ultraviolet light, which hardly exists under indoor illumination conditions.

Bismuth vanadate ($BiVO_4$) is yellow-colored semiconductor that has been widely used as a pigment, photoelectrochemical electrode and powdered photocatalyst [3-5].   One well-known powdered photocatalytic application for $BiVO_4$ is as an oxidation photocatalyst for water splitting in a Z-scheme reaction, and various kinds of $BiVO_4$ photocatalysts has been reported [6-10]. However, there have been only a few studies on photocatalytic decomposition of an organic compound by using $BiVO_4$, and dye decomposition reaction was used in most of those studies to evaluate photocatalytic activity [11-13].

The most decisive reason is that one-electron reduction of oxygen (O_2), which is a counterpart reaction of the oxidation of an organic compound by $BiVO_4$, is difficult due to its inferior conduction band potential (-0.06 ~ +0.02 V vs NHE, pH 0) [3,5,14].   Therefore, a semiconductor having a potential of the conduction band inferior to that of one-electron O_2 reduction (e.g., $O_2 + e^-$ = O_2^- (aq), -0.284 V vs NHE; $O_2 + H^+ + e^-$ = HO_2 (aq), -0.046 V vs NHE, pH 0) was believed to be inappropriate for photocatalytic organic decomposition.   Recently, several groups have resolved the problem of O_2 reduction by using a reduction cocatalyst.   In the case of tungsten(VI) oxide (WO_3), a reduction cocatalyst, e.g., platinum (Pt), palladium (Pd) or copper(II) oxide (CuO), induced multi-electron reduction of O_2 (e.g., $O_2 + 2H^+ + 2e^-$ = H_2O_2 (aq), +0.682 V vs NHE; $O_2 + 4H^+ + 4 e^-$ = $2H_2O$, +1.23 V vs NHE, pH 0), resulting in efficient oxidation of an organic compound under visible light irradiation [15-18].

Another reason for the inappropriateness of $BiVO_4$ for organic decomposition is the difficulty in synthesis of $BiVO_4$ particles with large specific surface area.   Although several methods for

preparing BiVO$_4$ have been reported, BiVO$_4$ with a specific surface area of only a few m^2 g^{-1} is obtained in almost all cases. Therefore, adsorption ability must be improved by a method other than increasing specific surface area, e.g., by composition of adsorbent materials. In the present study, we prepared a BiVO$_4$ nanocomposite photocatalyst with silica and a reduction cocatalyst, which increased adsorption and O$_2$ reduction ability, respectively.

2. Experimental

2.1. Sample preparation

2.1.1. Mesoporous silica

Silica was prepared by a previously reported method [19]. A solution containing 162.75 cm^3 of Milli-Q water, 8.5 cm^3 of hydrochloric acid, 5.56 cm^3 of buthanol and 4.5 g of Pluronic P123 (EO20PO70EO20, M_W =5800, Aldrich) was stirred for 1 h at 35 ^{o}C. Then 10.36 cm^3 of tetraethoxysilane was added to the solution. After stirring for 24 h at 35 ^{o}C, the solution was transferred into a Teflon bottle, and then the bottle sealed with a stainless jacket was heated at 100 °C for 24 h in an oven. After the hydrothermal treatment, the residue in the Teflon bottle was dried for 24 h at 100 ^{o}C and calcined for 3 h at 550 ^{o}C.

2.1.2. BiVO$_4$ with and without silica composition

BiVO$_4$ with silica composition was prepared by a previously reported method [13]. Three mmol of Bi(NO$_3$)$_3$•5H$_2$O and 3 mmol of NH$_4$VO$_3$ were added to 60 cm^3 of ethanol solution containing 3.0 cm^3 of nitric acid (69 wt%) under stirring. For BiVO$_4$ with silica composition, prepared silica was introduced into the solution, and then the mixture was sonicated for 100 min. The samples dried by heating for 24 h at 50 ^{o}C were calcined for 3 h at 400 ^{o}C, and BiVO$_4$ samples with and without silica composition were obtained.

2.1.3. Modification of Fe^{3+} by the impregnation method

An aqueous suspension composed of samples and an aqueous solution of iron(III) nitrate

(Fe(NO$_3$)$_3$) was stirred for 24 h.   After stirring, the supernatant and residue were separated by filtration, and the residue was washed with deionized water several times until the ionic conductivity of the supernatant was <10 μS cm^{-2} in order to remove NO$_3^-$ ions, and then the particles were dried under reduced pressure.

2.1.4. Loading of Pt by the photodeposition method

An aqueous suspension composed of particles and an aqueous ethanol solution (20 vol%) containing the corresponding amount of hexachloroplatinic acid (H$_2$PtCl$_6$•6H$_2$O) was photoirradiated with a light-emitting diode (LED; Lumileds, Luxeon LXHL-NRR8), which emitted light at a wavelength of ca. 455 nm with an intensity of 10 mW cm^{-2}, under a nitrogen atmosphere with vigorous magnetic stirring for 24 h.   After irradiation, photodeposited samples were obtained by washing with water several times and drying.

2.2. Characterization

Crystal structures of the particles were confirmed by using an X-ray diffractometer (Rigaku, MiniFlex II) with Cu Kα radiation (λ = 1.5405 Å).   The specific surface areas (S_{BET}) of the particles were measured by nitrogen adsorption on the basis of the Brunauer-Emmett-Teller equation with a surface area analyzer (Quantachrome, Nova 4200e).   The morphology of prepared particles was observed by scanning electron microscopy (SEM; JEOL, JSM-6701FONO) with energy dispersive X-ray spectroscopy (EDX; JEOL, JED-2300FONO)

2.3. Photocatalytic decomposition over acetaldehyde

Photocatalytic activities of samples were evaluated by photocatalytic decomposition of acetaldehyde.   One hundred milligrams of powder, which has complete extinction of incident radiation, was spread on a glass dish, and the glass dish was placed in a 125 cm^3 Tedlar bag (AS ONE Co. Ltd.).   Five hundred parts per million of gaseous acetaldehyde was injected into the Tedlar bag, and photoirradiation was performed at room temperature after the acetaldehyde had

reached an adsorption equilibrium.   The gaseous composition in the Tedlar bag was 79% N_2, 21% O_2, < 0.1 ppm of CO_2 and 500 ppm of acetaldehyde, and relative humidity was ca. 30%.   A 500-W xenon lamp (Ushio, SX-UI501XQ) was used as a light source and the wavelength of photoirradiation was controlled by L-42 filters (Asahi Techno Glass Co.), and an intensity of 120 mW cm^{-2} was used as the light source.   The concentrations of acetaldehyde and carbon dioxide (CO_2) were estimated by gas chromatography (Shimadzu, GC-8A, FID detector) with a PEG-20 M 20% Celite 545 packed glass column and by gas chromatography (Shimadzu, GC-9A, FID detector) with a TCP 20% Uniport R packed column and a methanizer (GL Sciences, MT-221), respectively. In the photocatalytic evaluation, a commercial $BiVO_4$ photocatalyst (Alfa Aesar Co., S_{BET} <1 m^2 g^{-1}) and commercial TiO_2, P-25 (Japan Aerosil Co., S_{BET} = 50 m^2 g^{-1}), were employed as standard photocatalysts.

3. Results and Discussion

3.1. Characterization of prepared samples

Figure 1 shows XRD patterns of $BiVO_4$ samples with and without silica composition.   Crystal structure of all $BiVO_4$ samples with silica composition was attributed to monoclinic-scheelite structure, and an appreciable difference depending silica content was not observed.   On the other hand, $BiVO_4$ without silica composition contained a trace amount of tetragonal-scheelite structure. Photocatalytic activity of $BiVO_4$ depending on crystal structure (monoclinic-scheelite, tetragonal-scheelite and tetragonal-zircon structure) has been studied, and it has been revealed that a monoclinic-scheelite structure showed higher photocatalytic activity for water oxidation under Z-scheme reaction and sacrificial electron reagent conditions [7].   Therefore, a monoclinic-scheelite structure is thought to be the most appropriate structure for photocatalytic reaction.

Figure 2 shows SEM images of $BiVO_4$ samples with and without silica composition. SEM-EDX analysis indicates that large spherical particles with particle size of 100 ~ 1000 nm were attributed to $BiVO_4$ and that smaller particles of silica were in close contact on the $BiVO_4$ surface.

Similar results for composite structure were obtained regardless of silica content.   Specific surface area greatly increased with an increase in the amount of silica.   These results indicate that increase in specific surface area was attributed not to change in $BiVO_4$ but to increase in the amount of silica. This is reasonable since the result because specific surface area of prepared silica was 700 m^2 g^{-1}, which was much larger than that of $BiVO_4$ without silica composition (2 m^2 g^{-1}).   However, the specific surface area of $BiVO_4$ with silica composition was smaller than the value calculated from experimental values of silica and $BiVO_4$.   This suggests that pores of silica were filled with $BiVO_4$ and thus the specific surface area of BiVO4 with silica composite decreased.

3.2. Photocatalytic activities of $BiVO_4$ samples with and without silica composition

Figure 3 shows results of photocatalytic evaluation of $BiVO_4$ samples with and without silica composition under visible light irradiation.   Prepared $BiVO_4$ without silica composition showed higher photocatalytic activity than that of commercial $BiVO_4$ because of its larger specific surface area, but the activity was not sufficiently high.   Photcatalytic reaction was increased by silica composition because adsorption ability was improved by a large increase in specific surface area. Concentration of acetaldehyde under an adsorption equilibrium in dark was decreased with increase of silica content, indicating that the silica assisted adsorption of acetaldehyde and improved photocatalytic activity (Table 1).

However, an excess amount of silica decreased photocatalytic activity.   This might be due to an insufficient amount of $BiVO_4$ photocatalyst.   For instance, $BiVO_4$ with 5 wt% silica composition contains 40 vol% silica and 60 vol% $BiVO_4$ (Table 1).   Thus, an excess amount of silica decreased photoabsorption and redox sites as a result of decrease in $BiVO_4$ photocatalyst.   Another possible reason for the decrease in photocatalytic activity is that it is difficult for acetaldehyde strongly adsorbed on the silica surface to diffuse to the surface of $BiVO_4$ and there was thus little oxidation of acetaldehyde on $BiVO_4$.

Although $BiVO_4$ with 5 wt% silica greatly improved photocatalytic activity, CO_2 generation was almost stopped before 500 ppm of CO_2 generation.   This is presumably attributed to the inferior

conduction band potential of $BiVO_4$ for one-electron O_2 reduction. Similar results were reported for WO_3, and the results were attributed to its inferior potential for one-electron O_2 reduction [15-18]. WO_3 can oxidize acetaldehyde to intermediate species, i.e., acetic acid, formaldehyde and formic acid, in the initial stage of reaction, but these intermediate species are not easily decomposed and accumulate on the surface [17,18]. In the case of WO_3, this problem was solved by using a reduction cocatalyst, e.g., Pt, Pd and CuO, which induced multi-electron reduction of O_2 [15-18]. In the present study, trivalent iron ion (Fe^{3+}) and Pt as reduction cocatalysts were loaded on $BiVO_4$ with an optimized amount of silica composition.

3.3. Photocatalytic activity of cocatalyst-loaded $BiVO_4$ with silica composition

Modification of Fe^{3+} has been reported to be effective for its utilization as a reduction cocatalyst for sulfur-doped TiO_2 [20-22]. Fe^{3+} induces efficient oxidation by accepting electrons, and generated Fe^{2+} recovers to Fe^{3+} by reacting with O_2. Our group proposed that Fe^{3+} modified on TiO_2 also acts as a sensitizer for visible light [23]. However, in the present case, Fe^{3+} on $BiVO_4$ possibly acted as an acceptor rather than a sensitizer for visible light because the number of photogenerated electrons in $BiVO_4$ under the present photocatalytic conditions was much larger than that in an Fe^{3+} compound.

Figure 4 shows results of photocatalytic evaluation of Fe^{3+}-mofified $BiVO_4$ with silica under visible light irradiation. Photocatalytic activity was improved by Fe^{3+} modification, and more than 500 ppm of CO_2 generation was observed. This indicates that multi-electron reduction of O_2 was induced by Fe^{3+}, thought a large increase in photocatalytic activity was not observed. One possible reason for this is that Fe^{3+} was adsorbed preferentially on the silica surface due to its large specific surface area.

For preferential loading of a cocatalyst on $BiVO_4$, Pt was loaded on $BiVO_4$ by the photodeposition method because Pt is expected to be mainly deposited on photoreduction sites (surface of $BiVO_4$). Figure 5 shows results of photocatalytic evaluation of Pt-loaded $BiVO_4$ with silica under visible light irradiation. Photodeposition of Pt greatly improved photocatalytic

activity, and CO_2 generation reached 1000 ppm, which means total decomposition of 500 ppm of acetaldehyde.   This is because Pt also induced multi-electron reduction of O_2 and efficient oxidation.   However, a large amount of Pt deposition decreased photocatalytic activity because an excess amount of Pt retards photoabsorption by covering the surface.

4. Conclusion

   A visible light response photocatalyst for photocatalytic organic decomposition was prepared by nanocomposition of $BiVO_4$, silica and reduction cocatalysts (Fe^{3+} and Pt).   Addition of silica increased photocatalytic activity as a result of improvement of adsorption ability. $BiVO_4$ with 5 wt % of silica composition showed the highest photocatalytic activity because of an optimized balance between adsorption ability and $BiVO_4$ amount.   Photodeposited Pt showed excellent cocatalytic performance, compared to Fe^{3+} modified by the impregnation method.   This is presumably because Pt was preferentially photodeposited on the surface of $BiVO_4$.

References

[1] A. Fujishima, T.N. Rao, D.A. Tryk, Titanium dioxide photocatalysis, J. Photochem. Photobiol. C: Photochem. Reviews 1 (2000) 1-21.

[2] M.R. Hoffmann, S.T. Martin, W. Choi, D.W. Bahnemann, Environmental applications of semiconductor photocatalysis, Chem. Rev. 95 (1995) 69-96.

[3] K. Sayama, A. Nomura, T. Arai, T. Sugita, R. Abe, M. Yanagida, T. Oi, Y. Iwasaki, Y. Abe, H. Sugihara, Photoelectrochemical decomposition of water into H_2 and O_2 on porous $BiVO_4$ thin-film electrodes under visible light and significant effect of Ag ion treatment, J. Phys. Chem. B 110 (2006) 11352-11360.

[4] Y.H. Ng, A. Iwase, A. Kudo, R. Amal, Reducing graphene oxide on a visible-light $BiVO_4$ photocatalyst for an enhanced photoelectrochemical water splitting, J. Phys. Chem. Lett. 1 (2010) 2607–2612.

[5] S.J. Hong, S. Lee, J.S. Jang, J.S. Lee, Heterojunction $BiVO_4$/WO_3 electrodes for enhanced photoactivity of water oxidation, Energy Environ. Sci. 4 (2011) 1781-1787.

[6] A. Kudo, K. Omori, H. Kato, A novel aqueous process for preparation of crystal form-controlled and highly crystalline $BiVO_4$ powder from layered vanadates at room temperature and its photocatalytic and photophysical properties, J. Am. Chem. Soc. 121 (1999) 11459-11467.

[7] S. Tokunaga, H. Kato, A. Kudo, Selective preparation of monoclinic and tetragonal $BiVO_4$ with scheelite structure and their photocatalytic properties, Chem. Mater. 13 (2001) 4624-4628.

[8] S. Sun, W. Wang, L. Zhou, H. Xu, Efficient methylene blue removal over hydrothermally synthesized starlike $BiVO_4$, Ind. Eng. Chem. Res. 48 (2009) 1735–1739.

[9] D. Ke, T. Peng, L. Ma, P. Cai, K. Dai, Effects of hydrothermal temperature on the microstructures of $BiVO_4$ and its photocatalytic O_2 evolution activity under visible light, Inorg. Chem. 48 (2009) 4685-4691.

[10] Y. Sasaki, H. Nemoto, K. Saito, A. Kudo, Solar water splitting using powdered photocatalysts driven by Z-schematic interparticle electron transfer without an electron mediator, J. Phys. Chem. C 113 (2009) 17536-17542.

[11] L. Zhang, D. Chen, X. Jiao, Monoclinic structured $BiVO_4$ nanosheets: hydrothermal preparation, formation mechanism, and coloristic and photocatalytic properties, J. Phys. Chem. B 110 (2006) 2668-2673.

[12] L. Zhou, W. Wang, L. Zhang, H. Xu, W. Zhu, Single-crystalline $BiVO_4$ microtubes with square cross-sections: microstructure, growth mechanism, and photocatalytic property, J. Phys. Chem. C 111 (2007) 13659-13664.

[13] G. Li, D. Zhang, J.C. Yu, Ordered mesoporous $BiVO_4$ through nanocasting: a superior visible light-driven photocatalyst, Chem. Mater. 20 (2008) 3983-3992.

[14] S. Kohtani, K. Yoshida, T. Maekawa, A. Iwase, A. Kudo, H. Miyabe, R. Nakagaki, Loading effects of silver oxides upon generation of reactive oxygen species in semiconductor photocatalysis, Phys. Chem. Chem. Phys. 10 (2008) 2986-2992.

[15] R. Abe, H. Takami, N. Murakami, B. Ohtani, Pristine simple oxides as visible light driven photocatalysts: Highly efficient decomposition of organic compounds over platinum-loaded tungsten oxide, J. Am. Chem. Soc., 130 (2008) 7780-7781.

[16] T. Arai, M. Horiguchi, M. Yanagida, T. Gunji, H. Sugihara, K. Sayama, Complete oxidation of acetaldehyde and toluene over a Pd/WO_3 photocatalyst under fluorescent- or visible-light irradiation, Chem. Commun. (2008) 5565-5567.

[17] T. Arai, M. Horiguchi, M. Yanagida, T. Gunji, S. Hideki, K. Sayama, Reaction mechanism and activity of WO_3-catalyzed photodegradation of organic substances promoted by a CuO cocatalyst, J. Phys. Chem. C 113 (2009) 6602–6609.

[18] T. Arai, M. Yanagida, Y. Konishi, Y. Iwasaki, H. Sugihara, K. Sayama, Promotion effect of CuO co-catalyst on WO_3-catalyzed photodegradation of organic substances, Catal. Commun. 9 (2008) 1254-1258.

[19] F. Kleitz, S.H. Choi, R. Ryoo, Cubic *I*a3d large mesoporous silica: synthesis and replication to platinum nanowires, carbon nanorods and carbon nanotubes, Chem. Commun. (2003) 2136–2137.

[20] T. Ohno, Z. Miyamoto, K. Nishijima, H. Kanemitsu, F. Xueyuan, Sensitization of photocatalytic activity of S- or N-doped TiO_2 particles by adsorbing Fe^{3+} cations, Appl. Catal. A:

Gen. 302 (2006) 62-68.

[21] K. Nishijima, B. Ohtani, X. Yan, T. Kamai, T. Chiyoya, T. Tsubota, N. Murakami, T. Ohno, Incident light dependence for photocatalytic degradation of acetaldehyde and acetic acid on S-doped and N-doped TiO_2 photocatalysts, Chem. Phys. 339 (2007) 64-72.

[22] T. Ohno, N. Murakami, T. Tsubota, H. Nishimura, Development of metal cation compound-loaded S-doped TiO_2 photocatalysts having a rutile phase under visible light, Appl. Catal. A: Gen. 349 (2008) 70-75.

[23] N. Murakami, T. Chiyoya, T. Tsubota, T. Ohno, Switching redox site of photocatalytic reaction on titanium(IV) oxide particles modified with transition-metal ion controlled by irradiation wavelength, Appl. Catal. A: Gen. 348 (2008) 148-152.

Table 1

Dependence of silica addition on specific surface area of $BiVO_4$ with silica composite estimated from results of the experiment (S_{BET}) and calculation (S_{cal}) and concentration of acetaldehyde under adsorption equilibrium (AcH_{eq}).

W_{ms} (wt%)	0	2	5	7.5	10	100
V_{ms}[a] (vol%)	0	20	40	50	58	100
S_{BET} ($m^2 g^{-1}$)	2	10	22	31	48	700
S_{cal}[b] ($m^2 g^{-1}$)		16	37	54	72	
AcH_{eq} (ppmv)	419	104	160	89	104	0

[a] Volume percent of mesoporous silica (V_{ms}) was calculated by using weight percent of mesoporous silica (W_{ms}), a pore volume (V_p) of $1.33\,cm^3\,g^{-1}$ for mesoporous silica KIT-6 [13], and densities (d_B and d_s) of 6.95 and $2.2\,g\,cm^{-3}$ for $BiVO_4$ and silica. Here, density for mesoporous (d_{ms}) silica can be calculated as follows: $d_{ms} = 1/(V_p + 1/d_s)$ [13]. Therefore, $V_{ms} = 100\,(W_{ms}/d_{ms})/[W_{ms}/d_{ms} + (100 - W_{ms})/d_B]$.

[b] S_{cal} can be calculated as follows: $S_{cal}(W_{ms}) = S_{BET}(W_{ms} = 0) + [S_{BET}(W_{ms} = 100) - S_{BET}(W_{ms} = 0)]\,W_{ms}/100$.
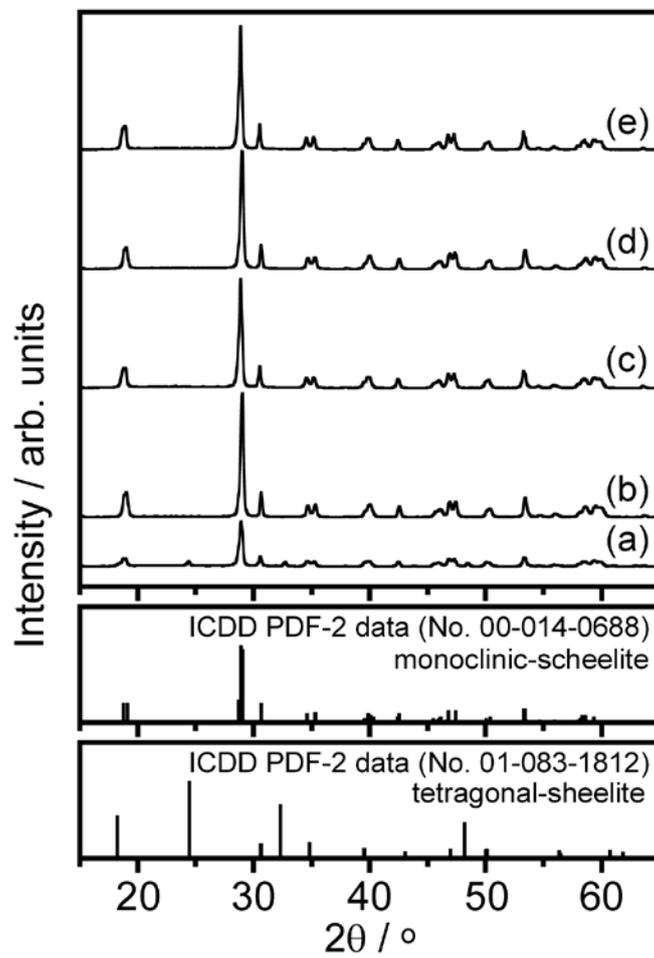
Figure 1. XRD patterns of BiVO$_4$ without (a) and with (b) 2 wt%, (c) 5 wt%, (d) 7.5 wt% and (e) 10 wt% of silica composition.
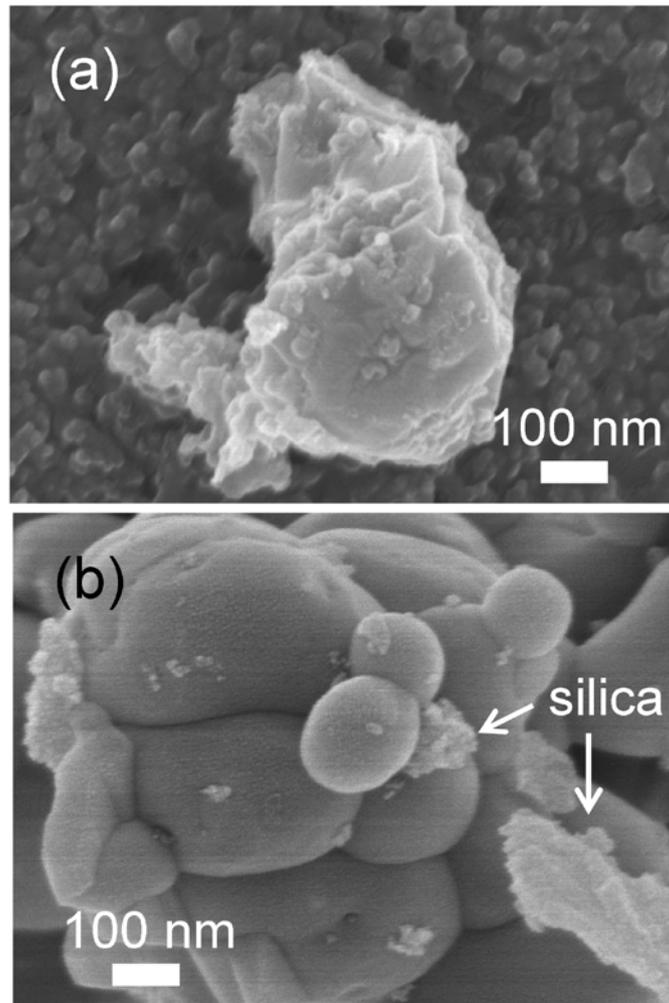
Figure 2. SEM images of (a) silica and (b) BiVO$_4$ with 5 wt% of silica composition.
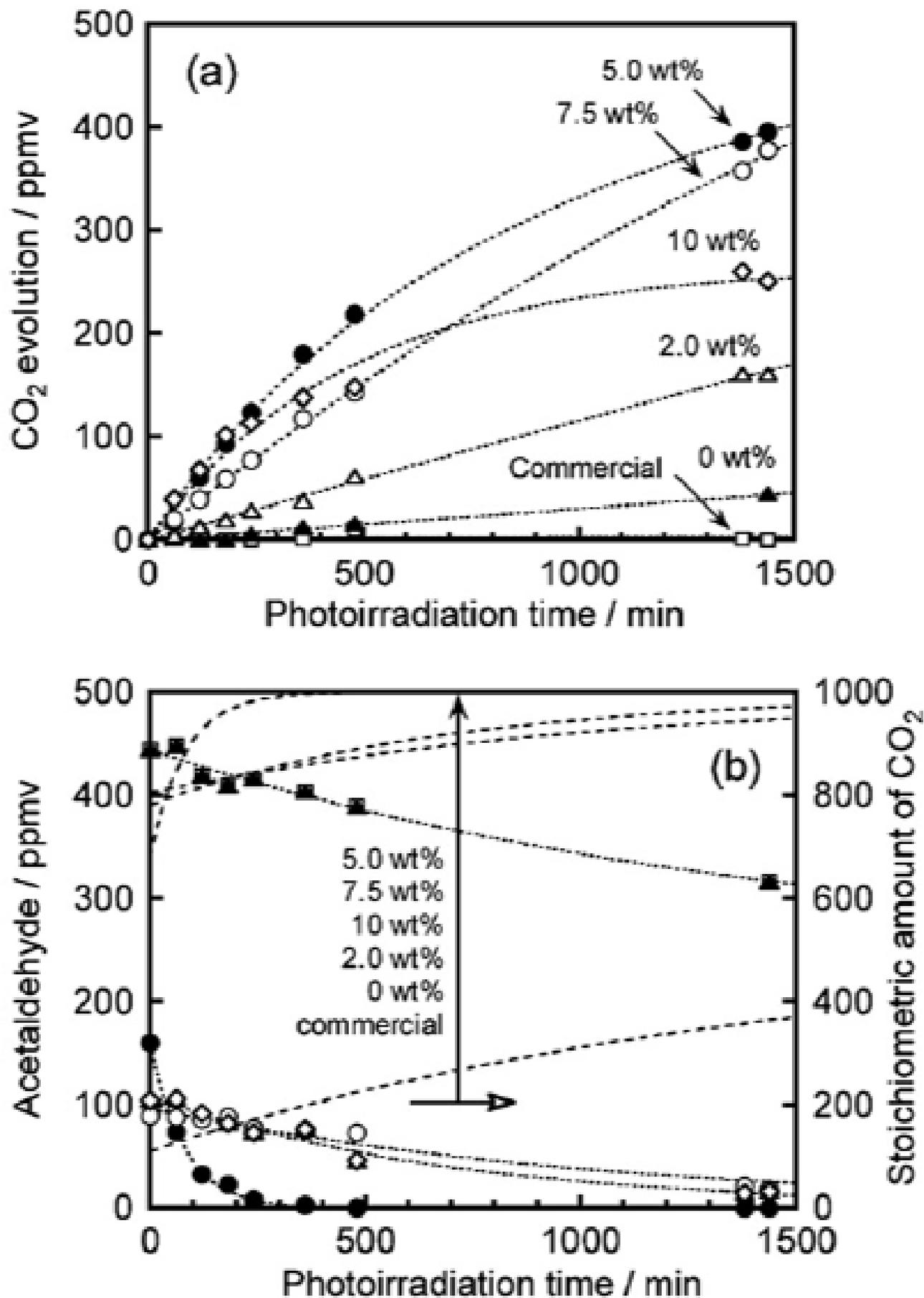
Fig. 3. Time courses of concentration of (a) CO_2 evolution and (b) acetaldehyde in gas phase over $BiVO_4$ with 0, 2, 5, 7.5 and 10 wt% of silica composition and commercial $BiVO_4$. Dashed lines in (b) shows stoichiometric amount of CO_2 calculated from decrease in acetaldehyde.
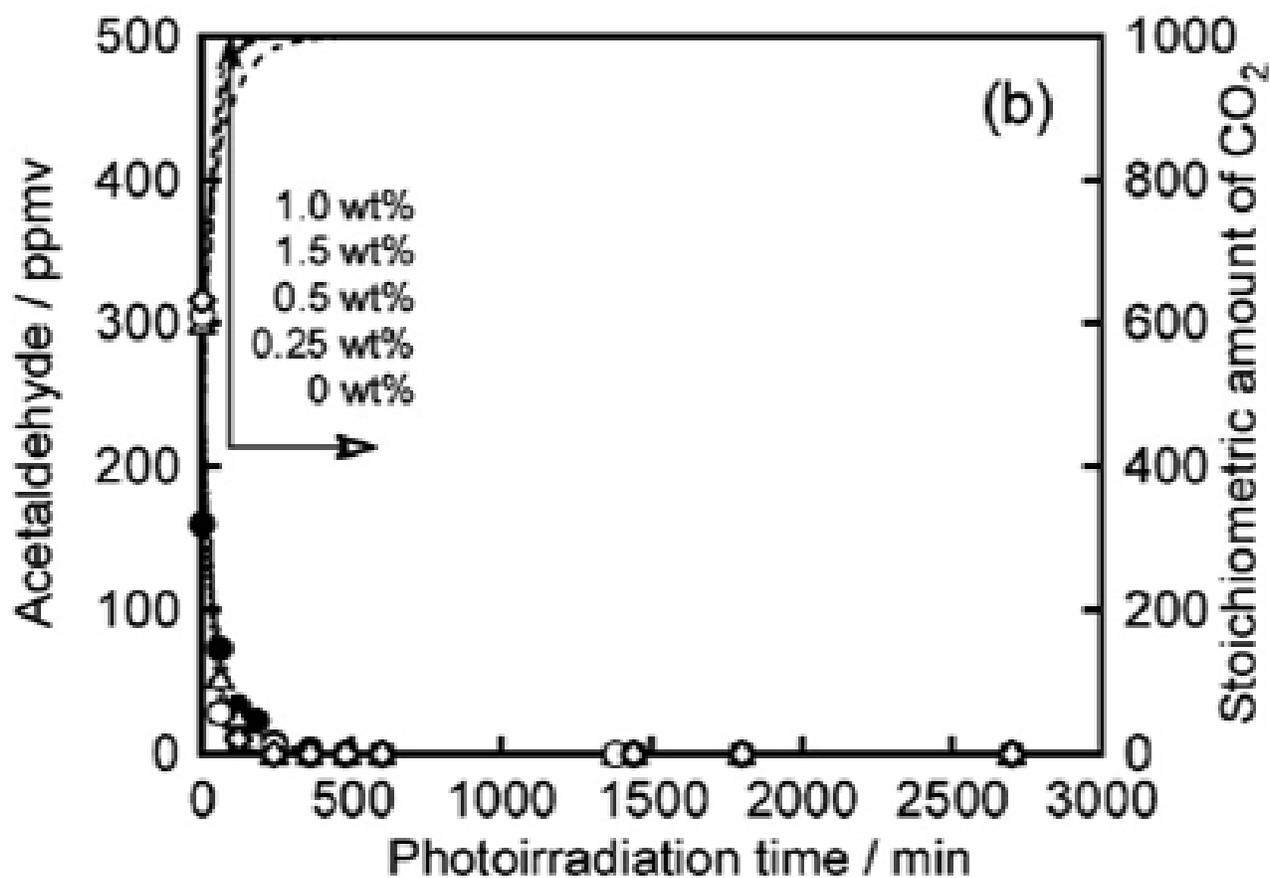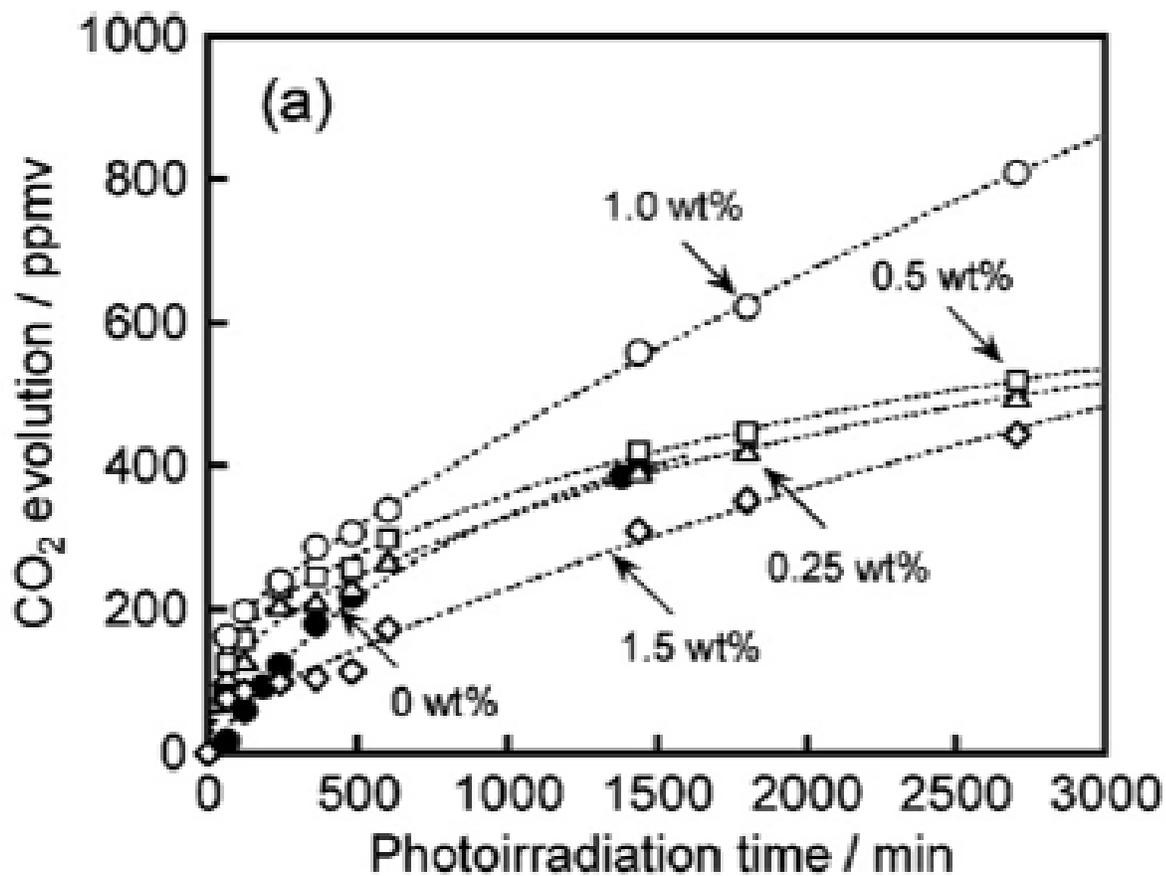
Fig. 4. Time courses of (a) CO_2 evolution and (b) acetaldehyde in gas phase over $BiVO_4$/silica composite with modification of 0, 0.25, 0.5, 1.0 and 1.5 wt% Fe^{3+}. Dashed lines in (b) shows stoichiometric amount of CO_2 calculated from decrease in acetaldehyde.
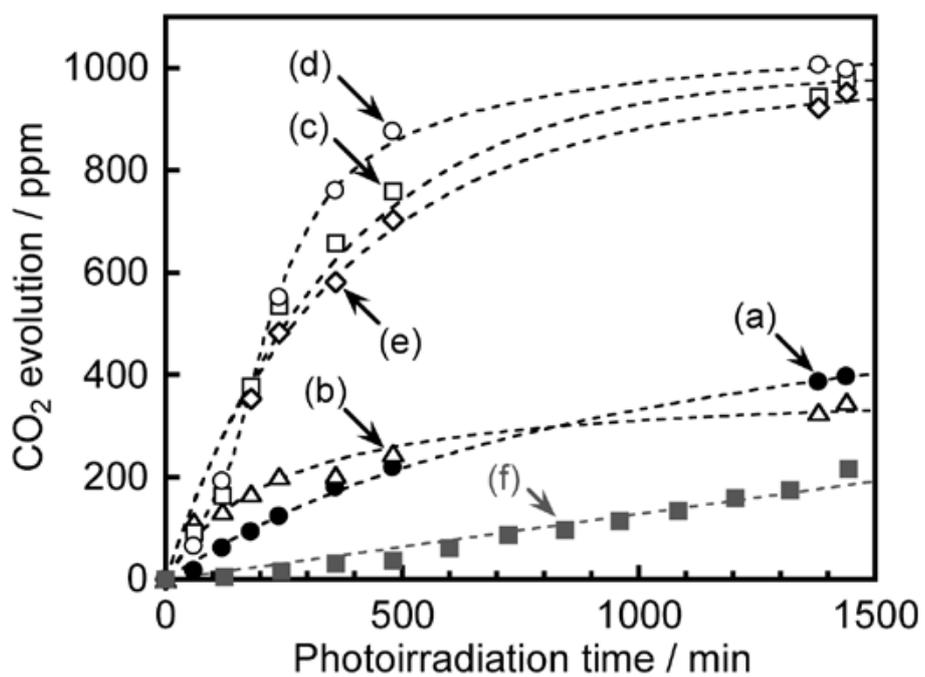
Figure 5. Time courses of CO_2 evolution of acetaldehyde decomposition over $BiVO_4$/silica composite without (a) and with photodeposition of (b) 0.5 wt%, (c) 0.75 wt%, (d) 1.0 wt% and (e) 2.0 wt% of Pt, and (f) commercial TiO_2, P-25.